Support information

Cobalt Vanadium Bimetallic Oxide Nanoplates Modified with RuO_2 for Efficient Electrocatalytic Overall Water Splitting

Yang Huang[a], Ying Gu[b]*, Jing Zhang[a], Bingyang Zhang[a], Dongxu Wang[a], Ying Xie[a], Aiping Wu[a]*, Chungui Tian[a]*

The content of Support information

Materials and Chemicals

All chemicals were of analytical grade and used without further purification. Deionized (DI) water was used in the experiments. Cobalt nitrate hexahydrate ($Co(NO_3)_2\cdot 6H_2O$)，Hydrated ruthenium chloride ($RuCl_3\cdot xH_2O$, >37% Ru) and Ruthenium oxide (RuO_2) were purchased from Shanghai Aladdin Chemical Reagent Co., Ltd. Ammonium vanadate (NH_4VO_3) was purchased from Tianjin Guangfu Science and Technology Development Co., Ltd. Hexamethynetetramine ($C_6H_{12}N_4$, HMT) was purchased from Shandong Xiya Chemical Industry Co., Ltd.

Physical Characterization

X-ray diffraction (XRD) patterns were recorded in Bruke D8 equipped with Cu-Ka (λ=1.5406 Å) radiation, and Rigaku Mini- flex600 diffractometer. Scanning Electron Microscopy (SEM) was carried out on ZEISS Sigma-500 instrument with accelerating voltage of 5kV. Transmission electron microscopy (TEM) and energy dispersive X-ray spectroscopy (EDS) elemental mapping characterizations were performed on JEM-F200 electron microscope (JEOL, Japan) with operating voltage of 200 kV. X-ray photon spectroscopy (XPS) analysis was carried out using a VG ESCALABMK II with Mg-Ka radiation (1253.6 eV).

Electrochemical measurements

All electrochemical measurements were performed on a CHI 760E electrochemical workstation at room temperature using a three-electrode system. Preparation of working electrodes: 5 mg of catalyst and 1 mg of carbon black were dispersed in 1 mL of a 1:1 (v/v) ethanol-water solvent mixture. Then, 30μL of Nafion (5 wt %, Sigma-Aldrich) was added to the mixture. The mixture was processed to produce a scattered slurry. The catalyst slurry was scraped onto treated nickel foam (1.0×1.0 cm^2) in alkaline and neutral solutions, and in acidic solution, the catalyst slurry was coated onto a carbon fiber paper (CP, (1.0×1.0 cm^2)). Then put it into a 60°C vacuum oven for drying and testing. Mercury oxide/saturated calomel electrode and graphite rods were used as reference and counter electrodes. The polarization curves were obtained following 20 cycles of cyclic voltammetry (CV) employing linear scanning voltammogram (LSV) evaluation at a scanning rate of 2 $mV \cdot s^{-1}$. The polarization curves were recorded according to $E_{RHE} = E_{HgO/Hg} + 0.059 \times pH + E^{\theta}_{HgO/Hg}$, and $E_{RHE} = E_{SCE} + 0.244\ V + 0.059pH$. All the reported potentials were converted to reversible Hydrogen Electrode (RHE). The electrochemical impedance spectra (EIS,0.01-100000 Hz, amplitude 5 mV) were measured at an overpotential using a current density of 10 mA cm^{-2}. The tafel plots were derived in the polarization curves. Cyclic voltammetry (CV) was measured in the non-faradaic potential region (0.1-0.2 V vs RHE for HER at a scan rate of 40 to 140 mV s^{-1}, 1.1-1.2 V vs RHE for OER at a scan rate of 20 to 60 mV s^{-1} to estimate the electrochemical double layer capacitance (C_{dl}). Double layer capacitance is known to be roughly proportional to electrochemically active surface area (ECSA). The ECSA was calculated from the following formula: ECSA = specific capacitance/40 μF cm^{-2} per cm^2. Specific capacitance is the calculated C_{dl}. 40 μF cm^{-2} is constant to convert capacitance to ECSA. The specific capacitance can be converted into electrochemical active surface area (ECSA) using the specific capacitance value for flat standard with 1 cm^2 of real surface area. A specific capacitance can be converted to an electrochemically active surface area by converting the specific capacitance to a specific capacitance value of a planar standard with a true surface area of 1 cm^2. Turnover frequency (TOF) was calculated by supposing every corresponding metal atom as active sites involved with catalytic reaction, showing as equation: TOF = jS/zFn. The Faraday efficiency (FE) is calculated by comparing the experimentally determined and theoretically calculated amounts of H_2 and O_2. In the experiment, constant potential electrolysis was performed in a closed h-type electrolytic cell at a rate of 53 mA cm^{-2} for 60 min. The amount of gas produced was analyzed by drainage method. The theoretical H_2/O_2 amount was calculated: n (H_2) = Q/nF where n(H_2), Q and F are the moles of hydrogen produced, the electrode charge and Faraday's constant (96485 $C \cdot mol^{-1}$), respectively. n is the number of electrons transferred during water splitting (for HER, n = 2, for OER, n = 4).

DFT calculations

Density Functional Theory (DFT) simulations are performed using the Cambridge Sequential Total Energy Package (CASTEP) module implemented in Material Studio.

The generalized gradient approximation (GG(A)) with Perdew-Burke-Ernzerhof (PBE) functionals was used to describe electron exchange and correlation effects, with a plane-wave energy cutoff set to 500 eV. To calculate the adsorption energies, we modeled a vacuum width of 15 Å. The free energy of adsorption of H* (ΔG_{H*}) is a valid descriptor of the activity of the HER, and catalysts with ΔG_{H*}= 0 are excellent candidates for the HER. The Gibbs free energy of H* (ΔG_{H*}) can be calculated from the equation ΔG_{H*} = $\Delta G_{H*} = \Delta E_{H*} + 0.24$ eV, where ΔE_{H*} is the adsorption energy of atomic hydrogen on a given unit cell. The models were optimized for convergence and the Gibbs free energy was calculated for each OER primary step. The adsorption behavior of each catalyst on *O, *OH and *OOH intermediates was simulated

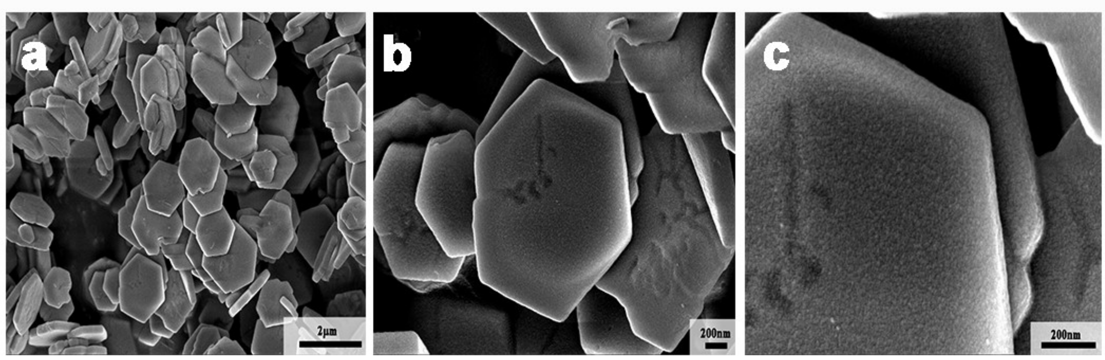

Figure S1. SEM images of CoVO-4.

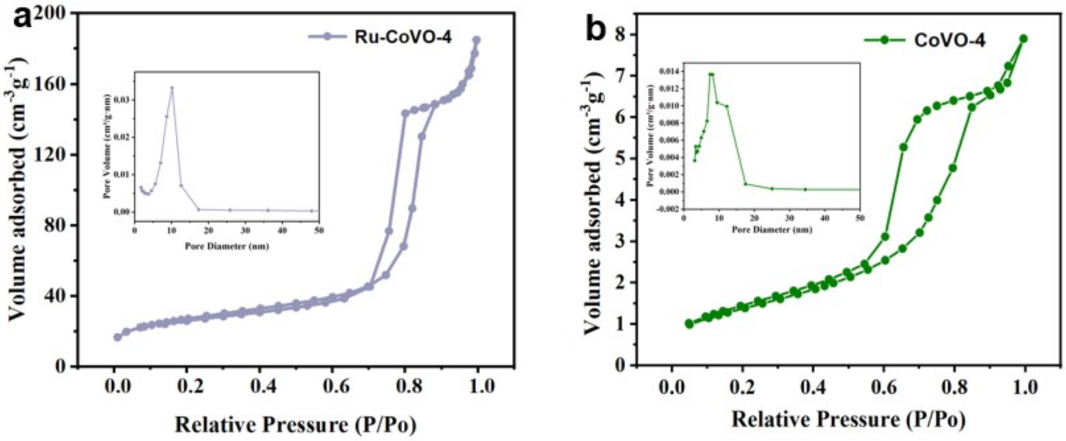

Figure S2. N_2 adsorption–desorption isotherm (Inset: pore size distribution) of (a)Ru-CoVO-4, (b) CoVO-4.

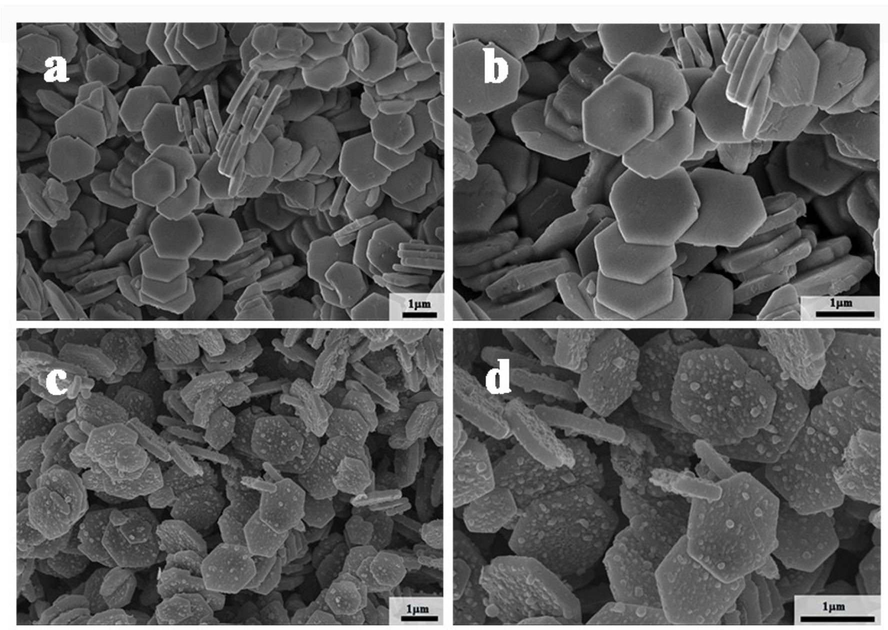

Figure S3. SEM images of (a-b) Ru-CoVO-3 and (c-d) Ru-CoVO-5.

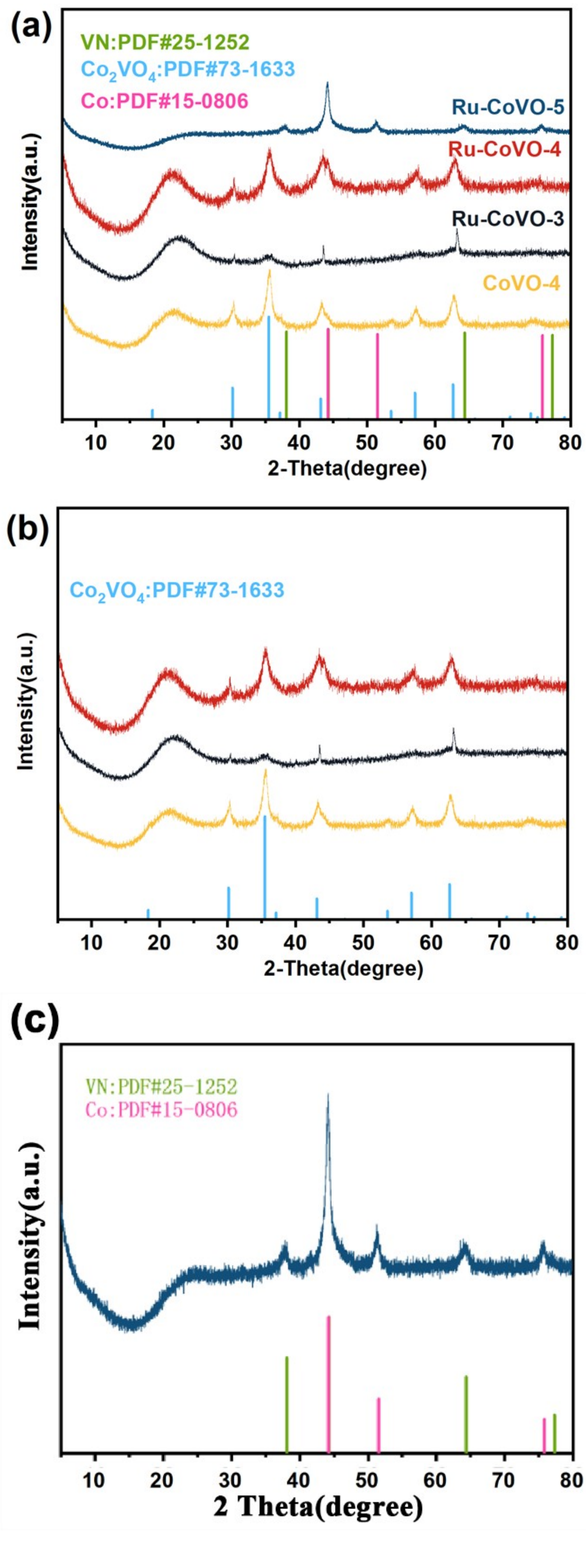

Figure S4. XRD patterns of Ru-CoVO-3, Ru-CoVO-5 and CoVO-4.

It can be seen from the figure that at 300°C and 400°C cobalt and vanadium are present in the form of the oxide CO_2VO_4. On increasing the temperature to 500°C, V combines with N to form VN and CO^{2+} is reduced to monomers, eventually forming CO/VN.

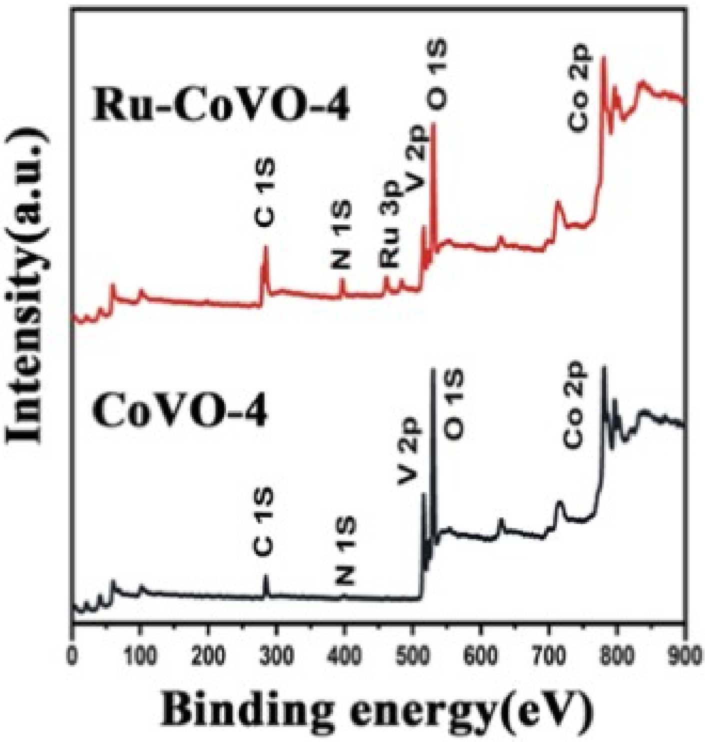

Figure S5. XPS spectra of Ru-CoVO-4 and CoVO-4.

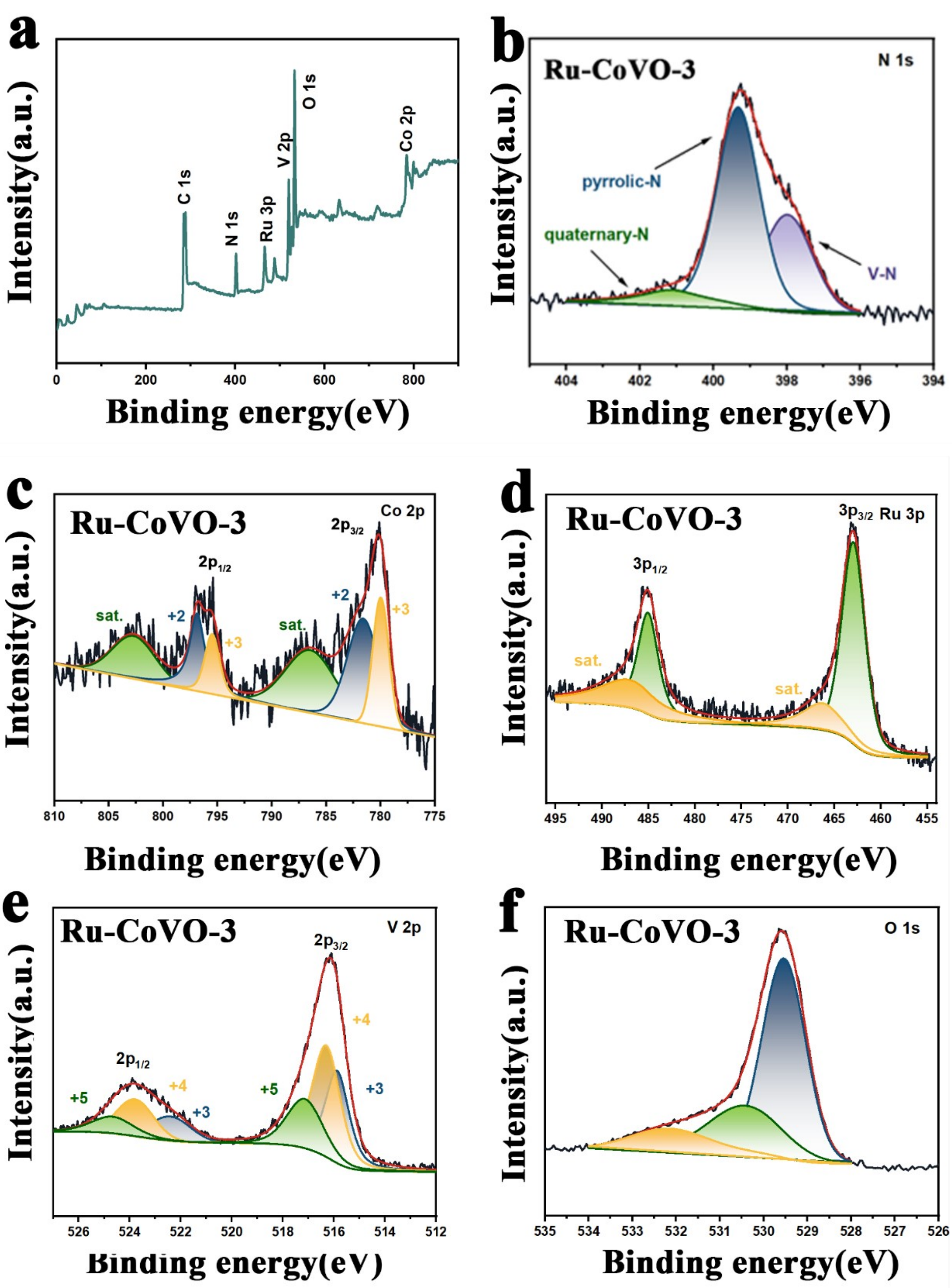

Figure S6. XPS spectra of Ru-CoVO-3.

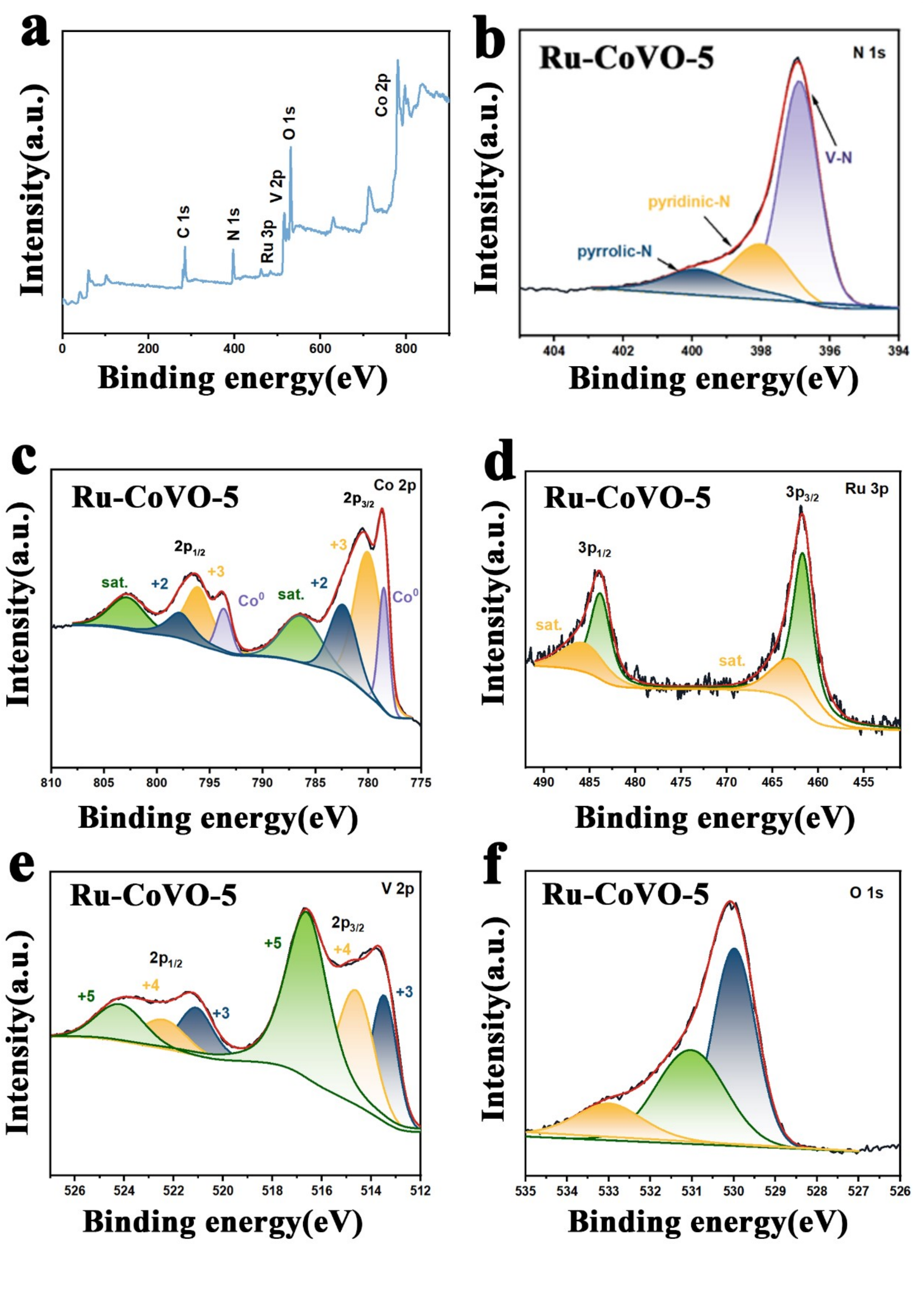

Figure S7. XPS spectra of Ru-CoVO-5.

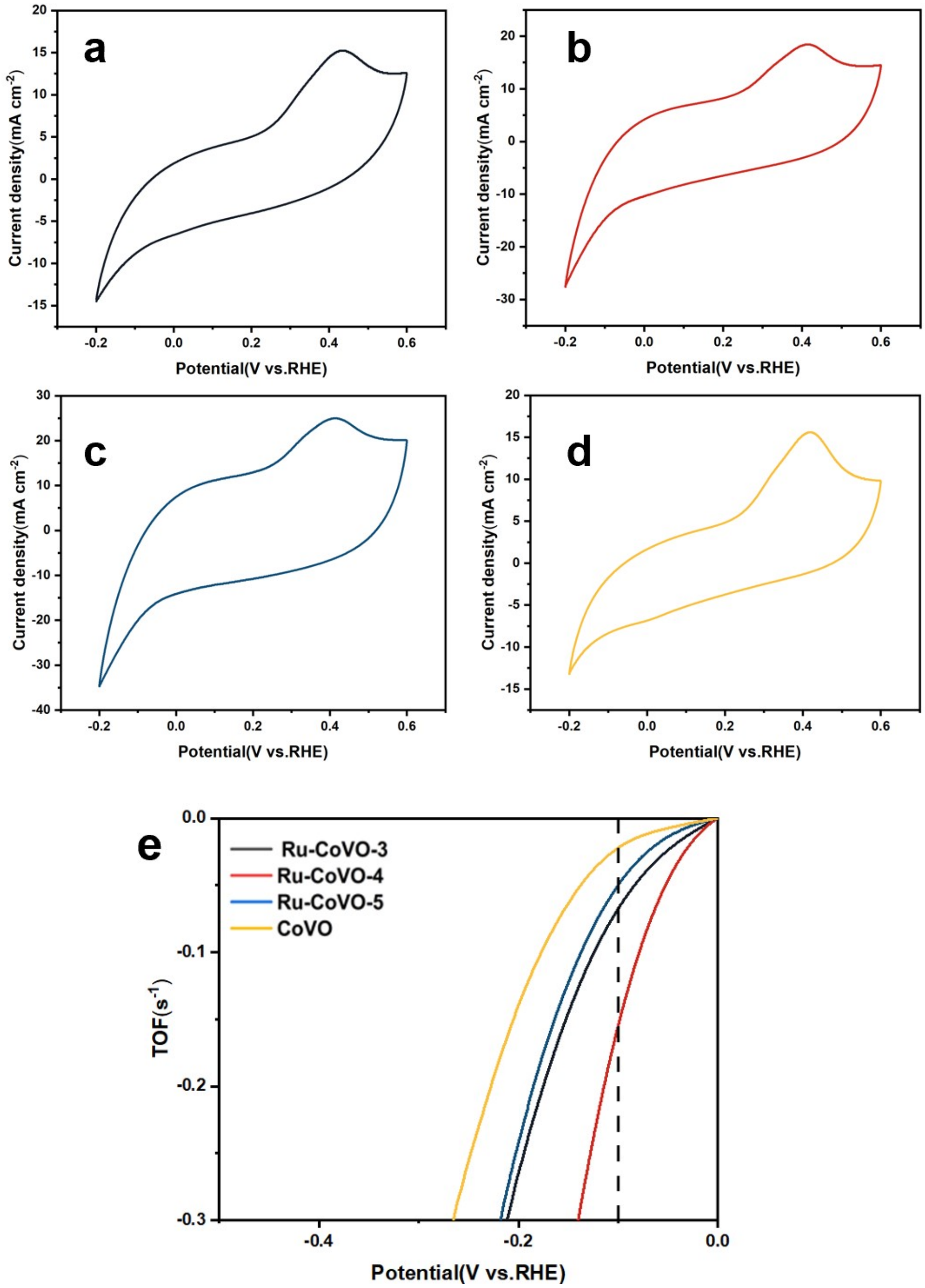

Figure S8. (a-d) CVs of Ru-CoVO-3, Ru-CoVO-4, Ru-CoVO-5, and CoVO-4 scanned at a rate of 50 mV s^{-1} in 1 M phosphate buffer (PBS, PH=6.9). (e) Calculated TOF for Ru-CoVO-3, Ru-CoVO-4, Ru-CoVO-5, and CoVO-4 in 1 M KOH.

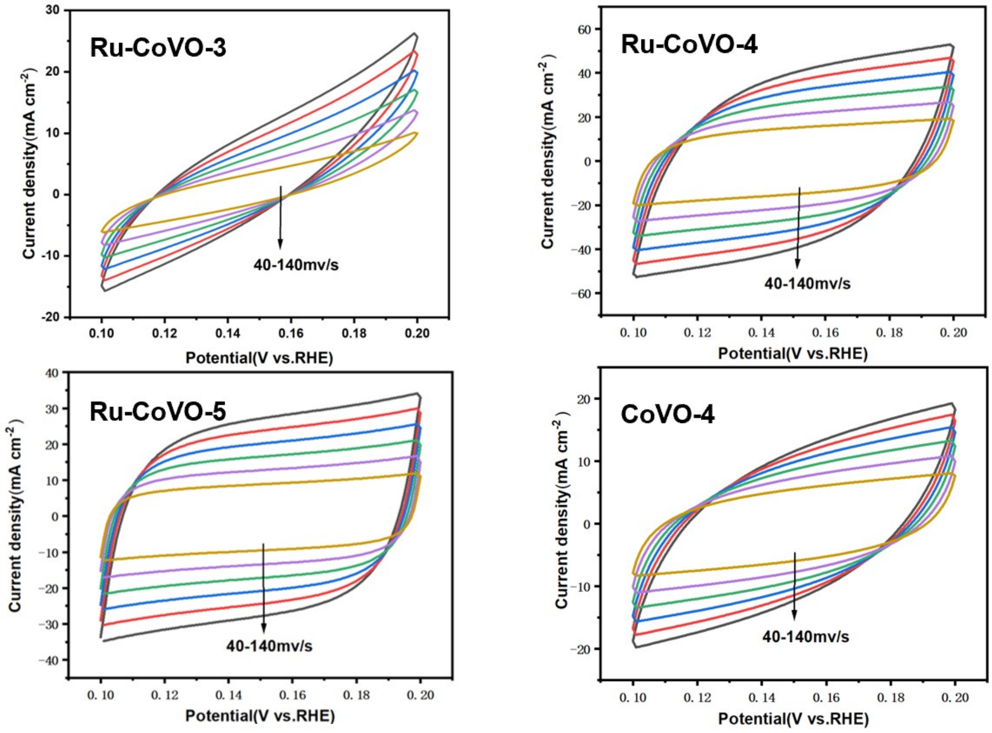

Figure S9. CVs within the potential range of 0.1 to 0.2 V vs. RHE in 1 M KOH at the different scan rates from 40 to 140 mV s^{-1} for Ru-CoVO-3、Ru-CoVO-4、Ru-CoVO-5 and CoVO-4.

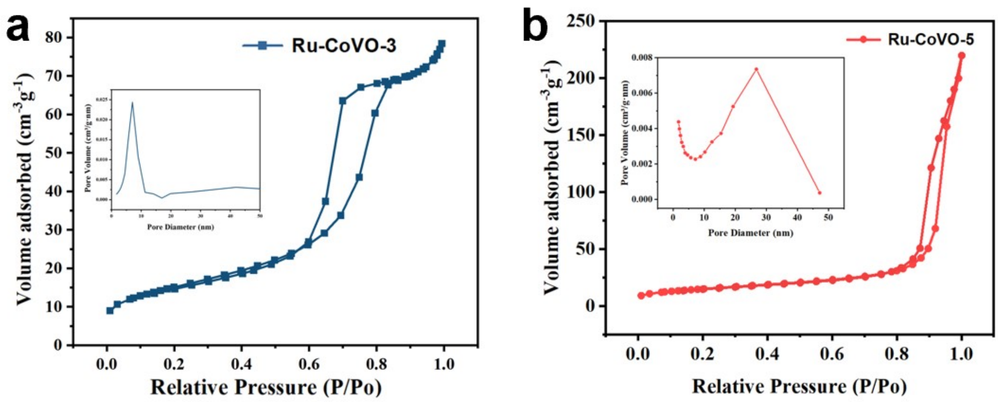

Figure S10. N_2 adsorption–desorption isotherm (Inset: pore size distribution) of (a) Ru-CoVO-3, (b) Ru-CoVO-5.

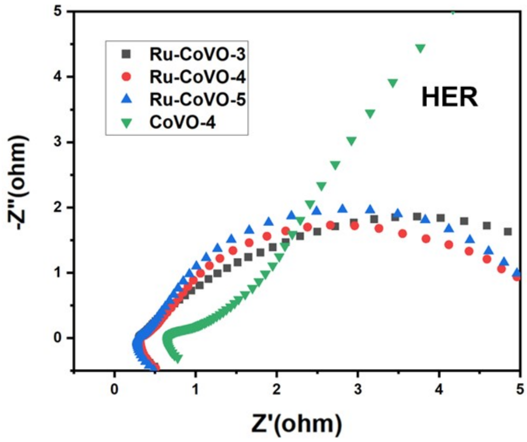

Figure S11. HER EIS Nyquist plots (original experimental data) of different electrocatalysts in 1M KOH.

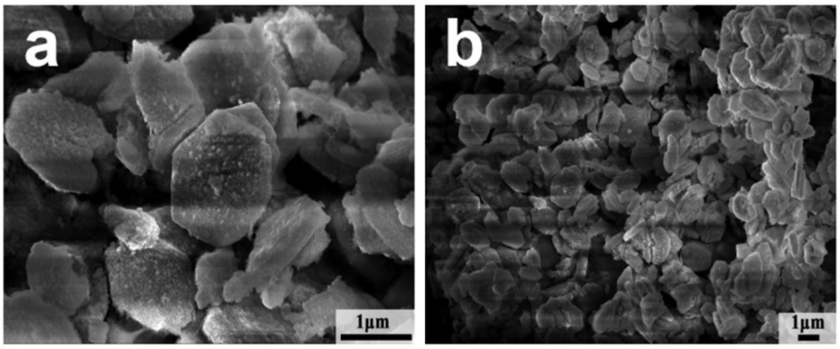

Figure S12. (a-b) SEM images of Ru-CoVO-4 after stability test for HER in 1M KOH.

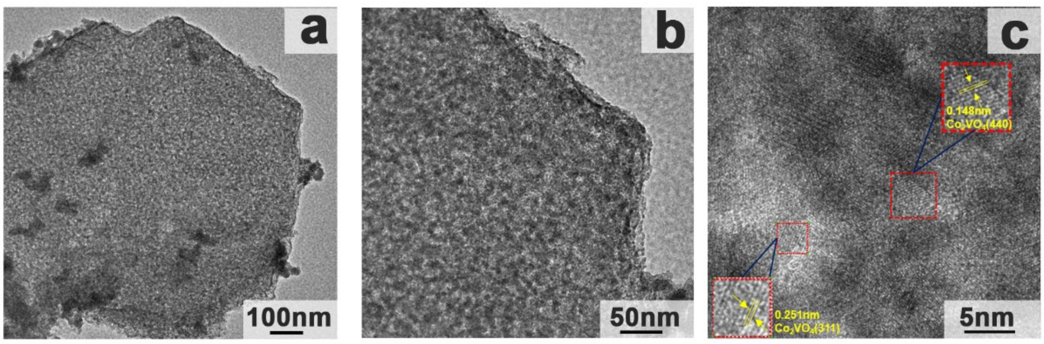

Figure S13. (a-c) TEM images of Ru-CoVO-4 after stability test for HER in 1M KOH.

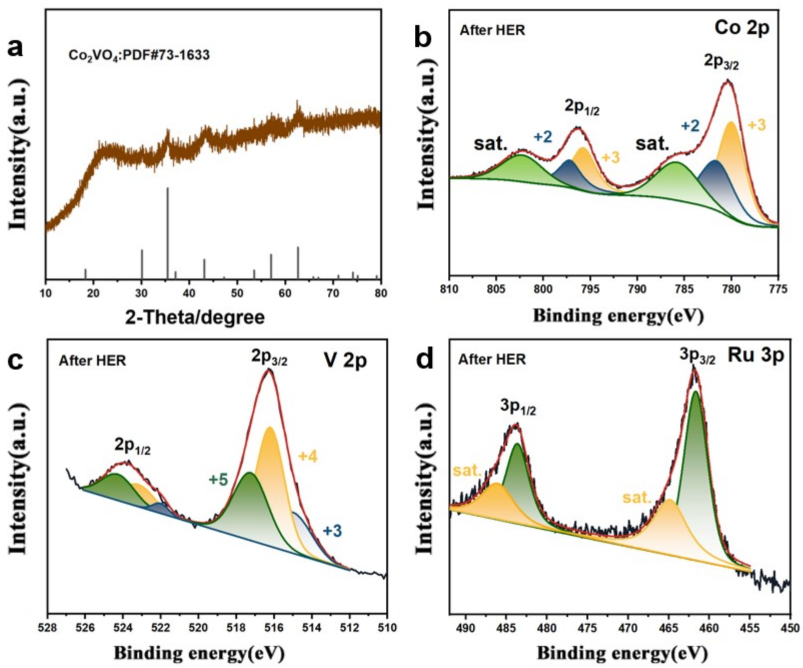

Figure S14. (a)XRD pattern of the Ru-CoVO-4 after the stability test. (b-d) XPS spectra of Ru-CoVO-4 after stability test.

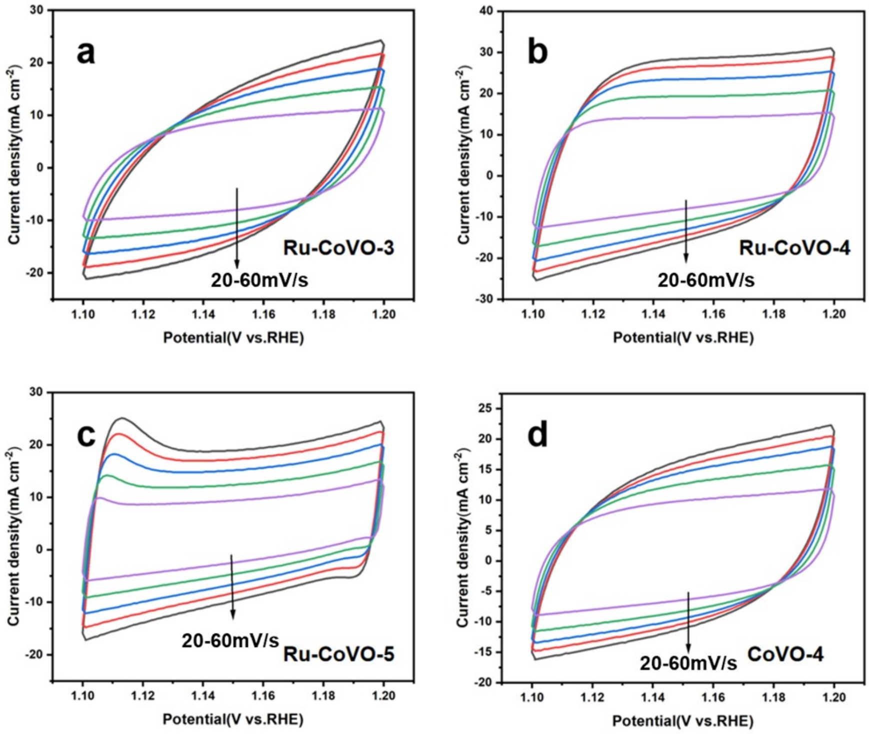

Figure S15. CVs within the potential range of 1.10 to 1.20 V vs. RHE in 1 M KOH at the different scan rates from 20 to 60 mV s^{-1} for Ru-CoVO-3, Ru-CoVO-4, Ru-CoVO-5 and CoVO-4.

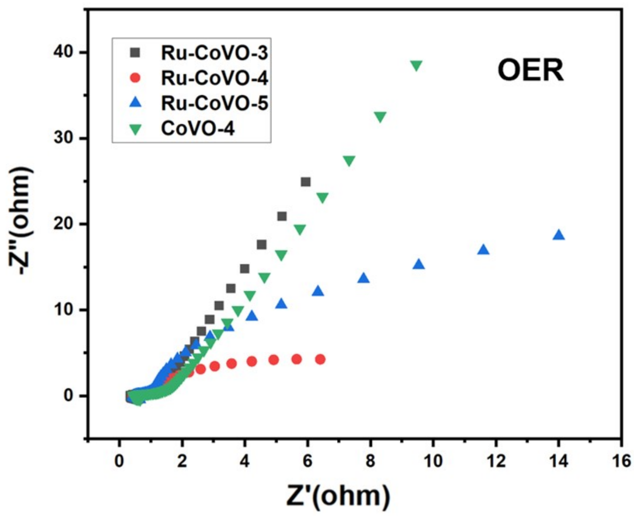

Figure S16. OER EIS Nyquist plots (original experimental data) of different electrocatalysts in 1M KOH.

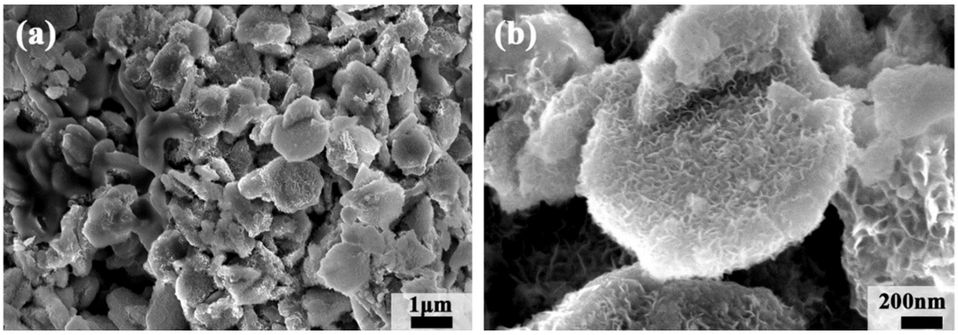

Figure S17. (a-b) SEM image of Ru-CoVO-4 (after stability test in 1M KOH-OER 60h).

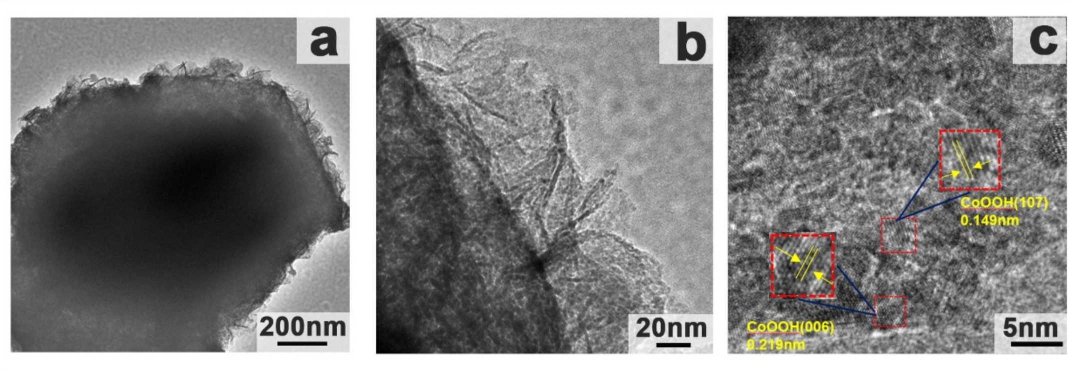

Figure S18. (a-c) TEM images of Ru-CoVO-4 after stability test for OER in 1M KOH.

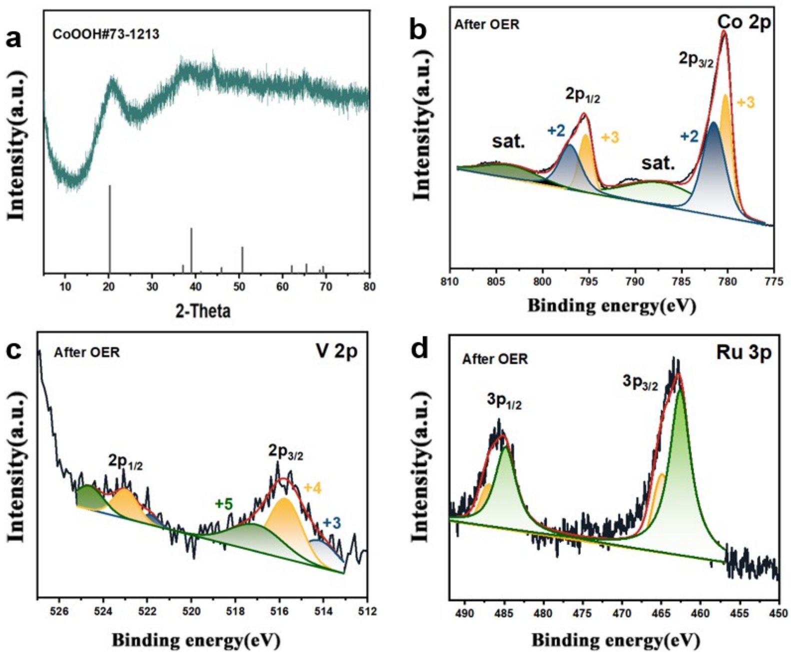

Figure S19. (a)XRD pattern of the Ru-CoVO-4 after the stability test. (b-d) XPS spectra of Ru-CoVO-4 after stability test.

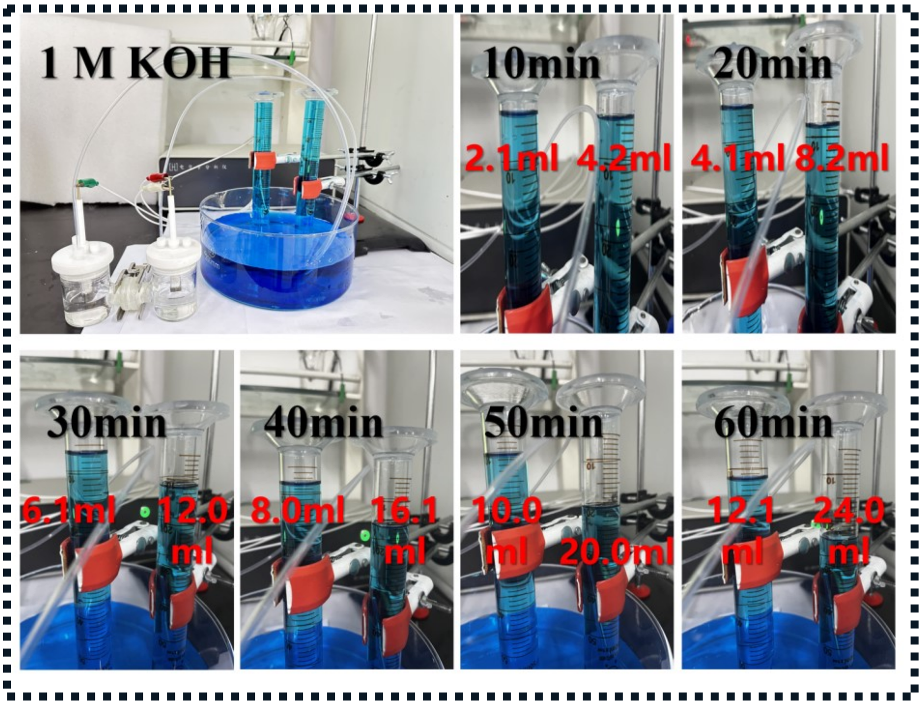

Figure S20. Digital photographs of H-type electrolyzer employing Ru-CoVO-4 as both anodic and cathodic catalysts and the gas collection device using drainage method.

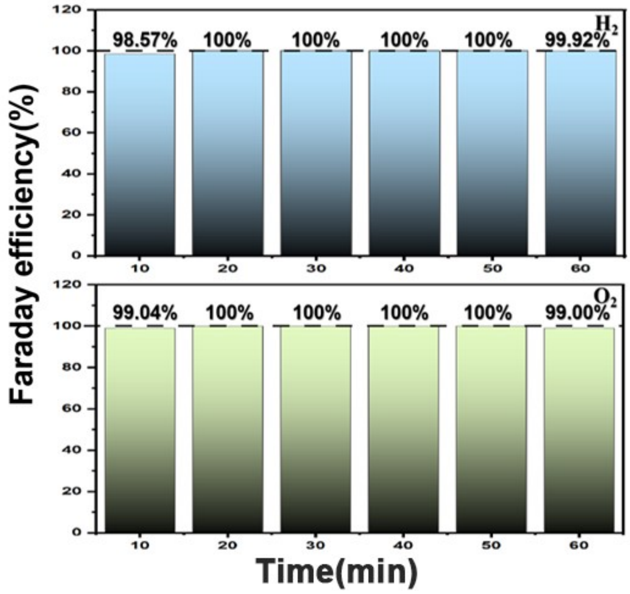

Figure S21. Faradaic efficiency of Ru-CoVO-4 under different operating times.

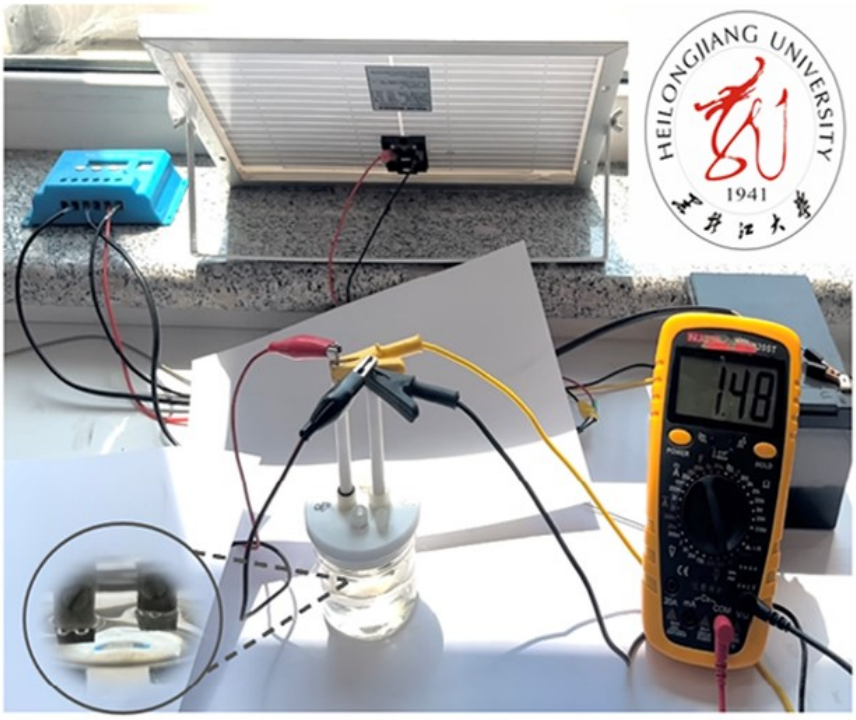

Figure S22. Photograph of solar panel assisted water splitting device.

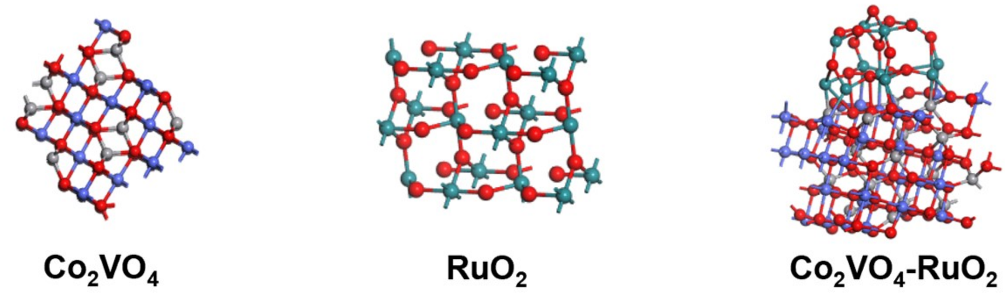

Figure S23. The models of Co_2VO_4， RuO_2， Co_2VO_4-RuO_2.

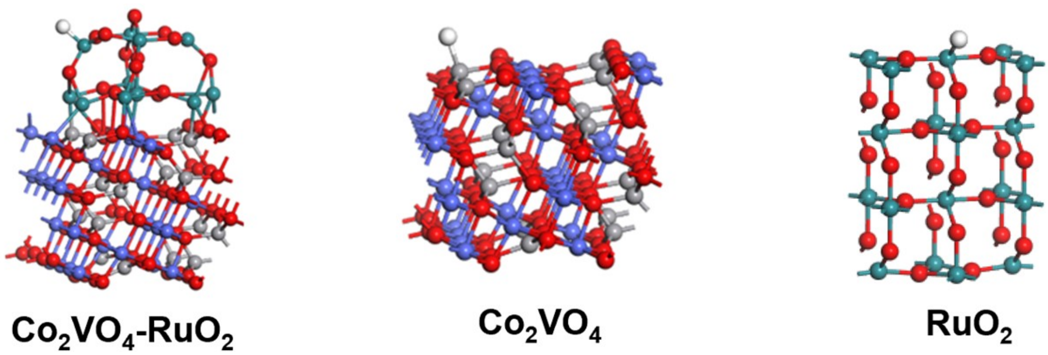

Figure S24. Optimized hydrogen adsorption sites.

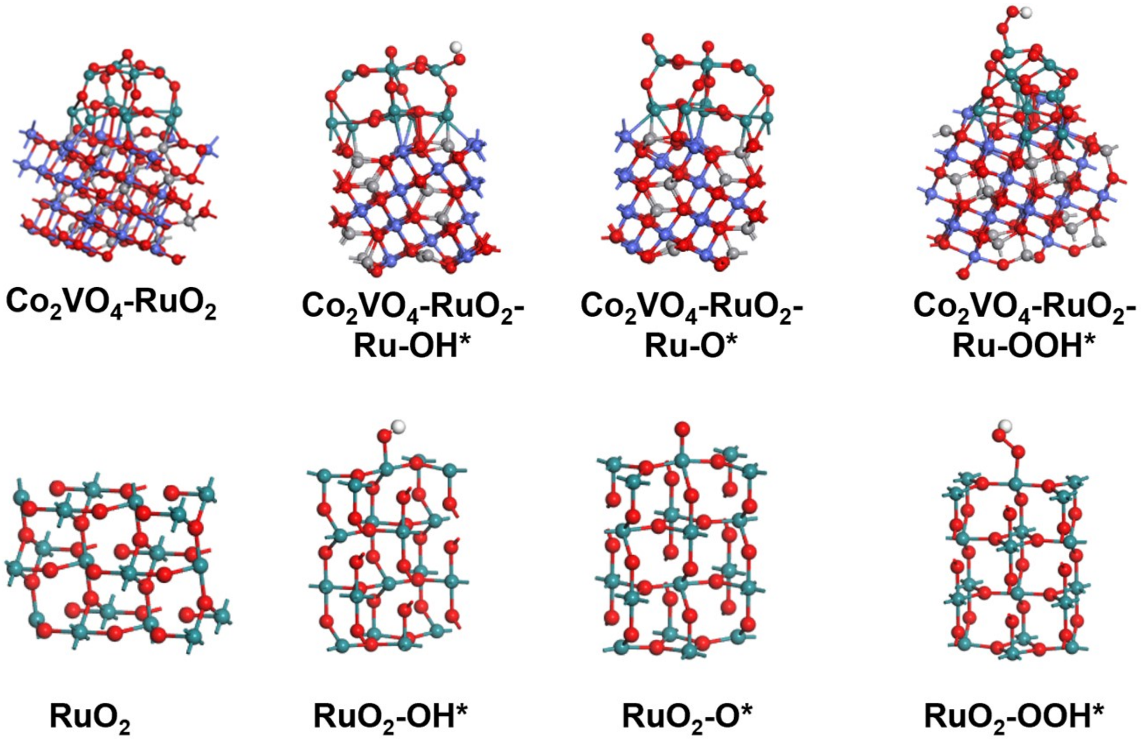

Figure S25. The models of Co_2VO_4-RuO_2 and RuO_2 with potential OH*, O*, OOH* adsorbed on its surface, respectively.

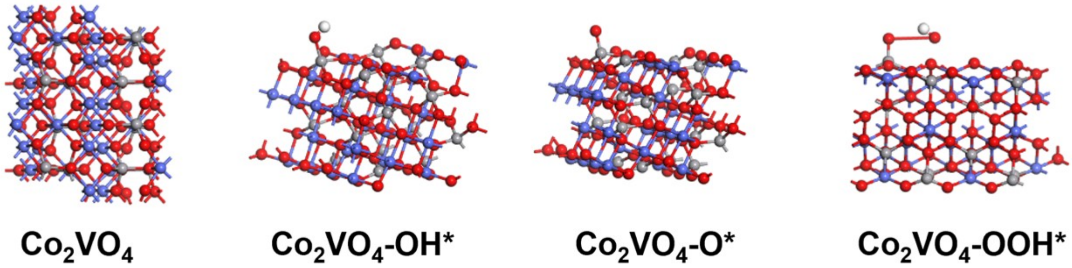

Figure S26. The models of Co_2VO_4 with potential OH*, O*, OOH* adsorbed on its surface, respectively.

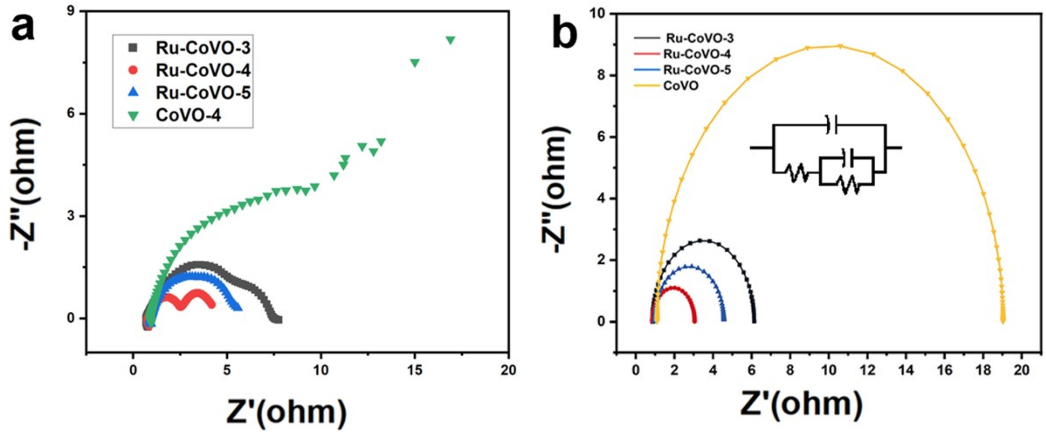

Figure S27. Corresponding Nyquist plots (a) original experimental data and (b) simulated data of different electrode for HER in 0.5M H_2SO_4.

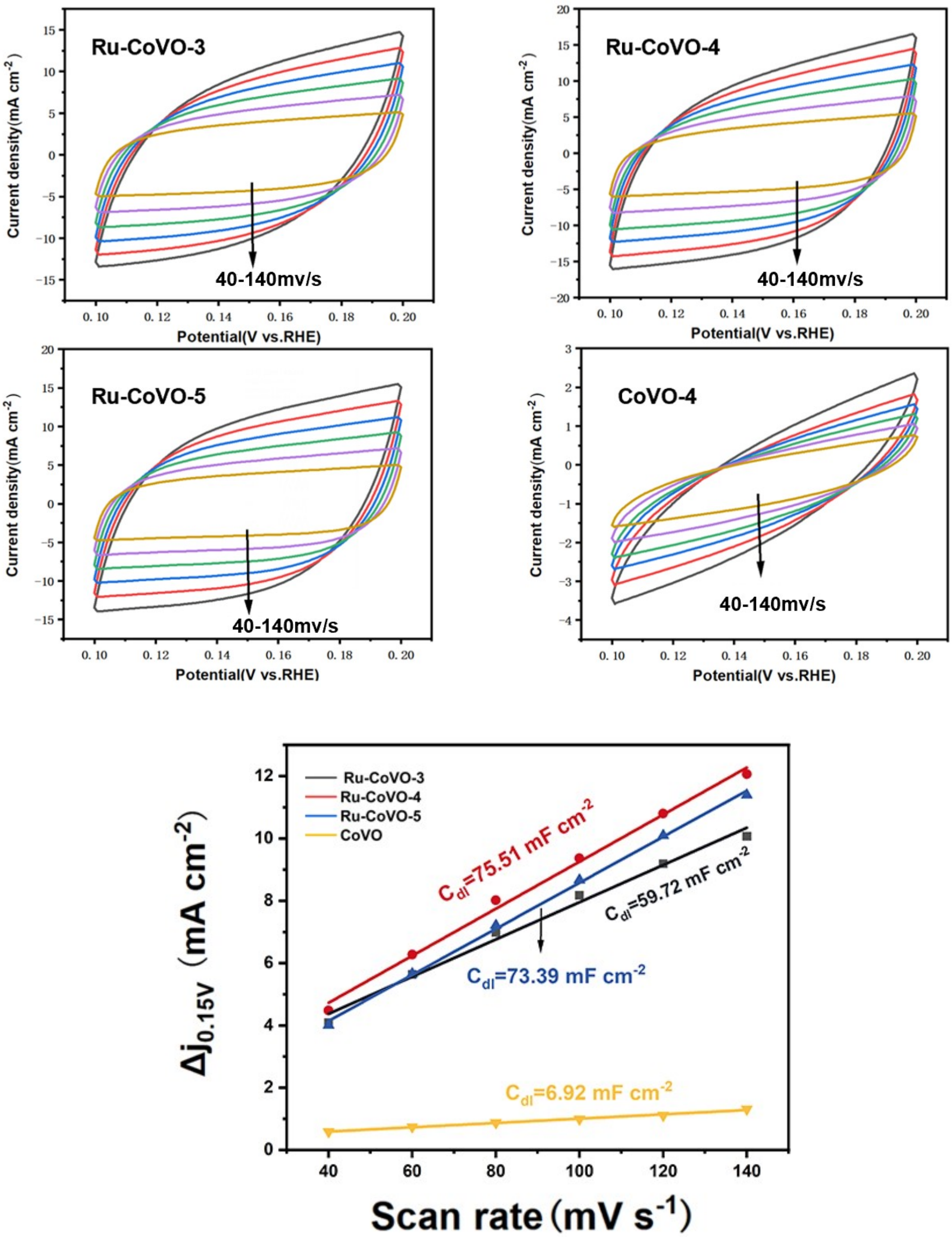

Figure S28. CVs within the potential range of 0.1 to 0.2 V vs. RHE in 0.5 M H_2SO_4 at the different scan rates from 40 to 140 mV s^{-1} for Ru-CoVO-3, Ru-CoVO-4, Ru-CoVO-5 and CoVO-4; Plots showing extraction of the double-layer capacitance (C_{dl}).

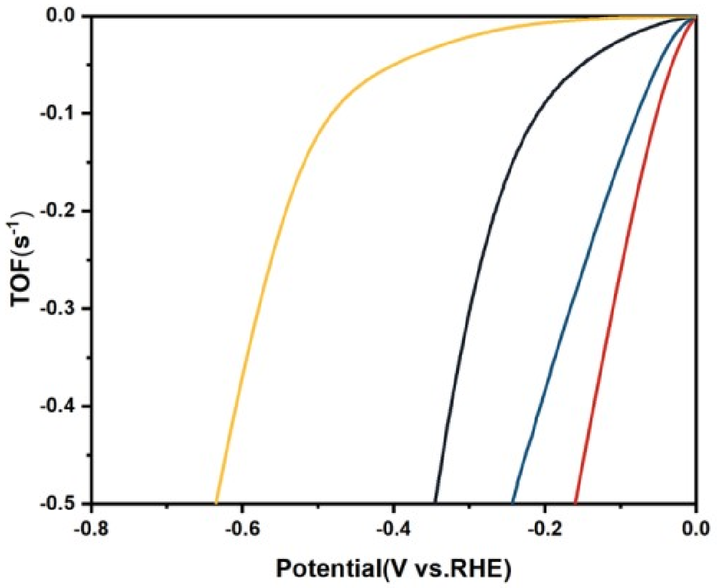

Figure S29. Calculated TOF for Ru-CoVO-3, Ru-CoVO-4, Ru-CoVO-5, and CoVO-4 in 0.5 M H_2SO_4.

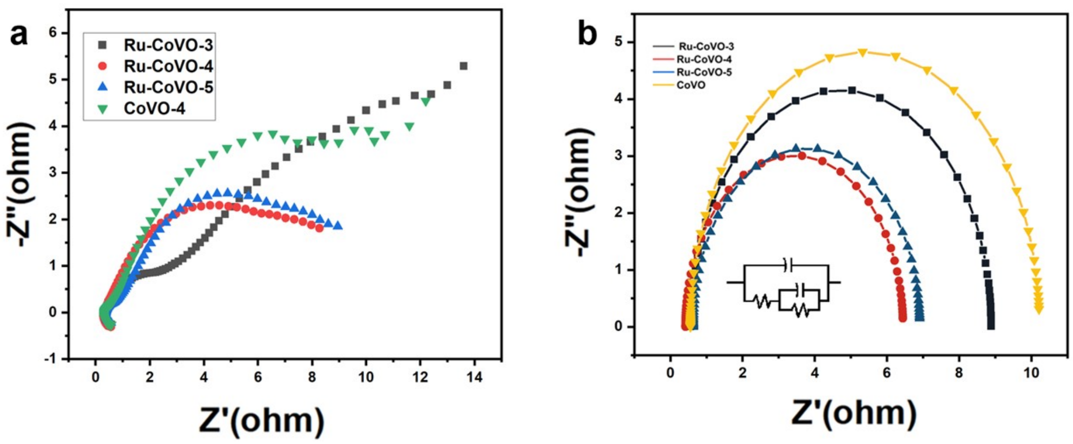

Figure S30. Corresponding Nyquist plots (a) original experimental data and (b) simulated data of different electrode for HER in 1M PBS.

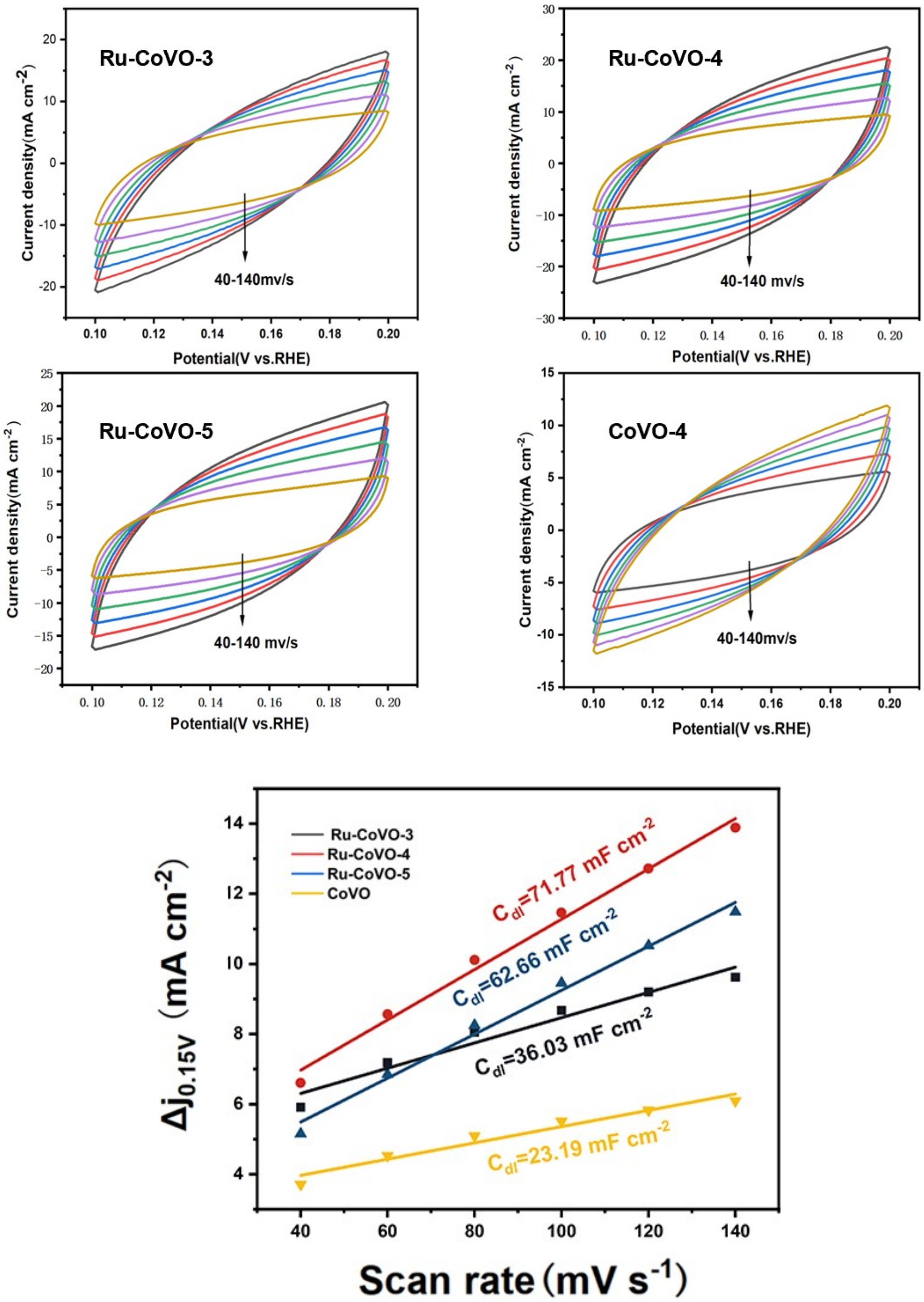

Figure S31. CVs within the potential range of 0.1 to 0.2 V vs. RHE in 1 M PBS at the different scan rates from 40 to 140 mV s^{-1} for Ru-CoVO-3, Ru-CoVO-4, Ru-CoVO-5 and CoVO-4; Plots showing extraction of the double-layer capacitance (C_{dl}).

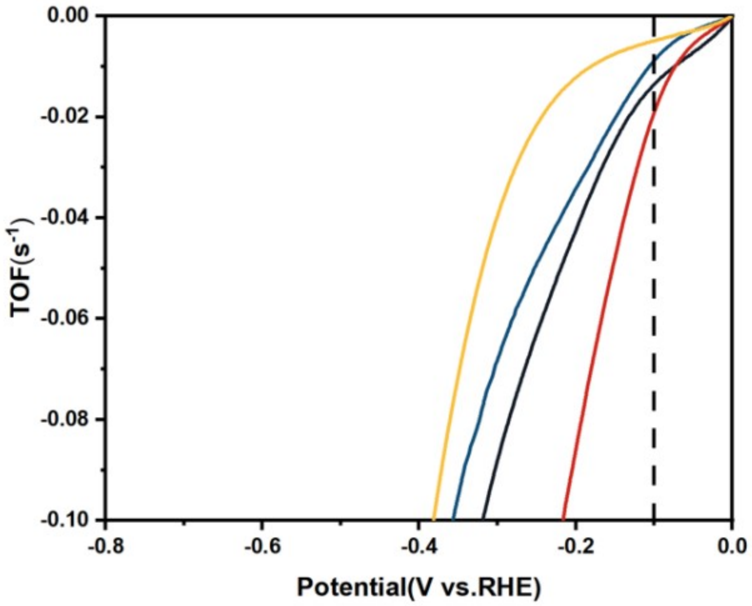

Figure S32. Calculated TOF for Ru-CoVO-3, Ru-CoVO-4, Ru-CoVO-5, and CoVO-4 in 1 M PBS.

Table S1. Metal content of various catalysts analysed by ICP-AES measurements.

sample	Temperature (°C)	Ru content(%)	Co content(%)	V content(%)
Ru-CoVO-3	300	1.9%	19.3%	13.7%
Ru-CoVO-4	400	2.1%	29.4%	20.2%
Ru-CoVO-5	500	1.8%	21.2%	15.5%

Table S2. Comparison of recently reported electrocatalysts for HER in 1 M KOH.

HER catalysts	Electrolyte	η_{10} (mV)	Tafel slope ($mV\cdot dec^{-1}$)	Reference
Ru-CoVO-4	1 M KOH	49	59.69	This work
Ru/EG-rGO-114	1 M KOH	54	35	C.-K. Hung, A. R. Thiruppathi, N. Burns, C. McGuire, J. Quintal, D.-T. Jiang, S. Kycia and A. Chen, *Acs Catalysis*, 2024, **14**, 5416-5428.
Ru@RuO_2-250	1 M KOH	32	21.7	Z. Li, J. Zou, T. Liang, X. Song, Z. Li, J. Wen, M. Peng, X. Zeng, H. Huang and H. Wu, *Chemical Engineering Journal*, 2023, **460**, 141672.
RuNi-0	1 M KOH	69	73	N. Liu, Z. Zhai, B. Yu, W. Yang, G. Cheng and Z. Zhang, *International Journal of Hydrogen Energy*, 2022, **47**, 31330-31341.
Ru-Ni/Co	1 M KOH	59	64	L. Li, H. Qiu, Y. Zhu, G. Chen, S. She, X. Guo, H. Li, T. Liu, Z. Lin, H. Zhou, Y. Zhu, M. Yang, B. Xu and H. Huang, *Applied Catalysis B: Environmental*, 2023, **331**, 122710.
$Ru_{0.10}$@2H-MoS_2	1 M KOH	51	64.9	J. Wang, W. Fang, Y. Hu, Y. Zhang, J. Dang, Y. Wu, B. Chen, H. Zhao and Z. Li, *Applied Catalysis B: Environmental*, 2021, **298**, 120490.
Ru_3–TiO_2 NWAs/CC	1 M KOH	61	47.4	S. Wang, L. Sang, F. Zhang, Y. Li, B. Xu, P. Zhang, B. Liu and Y. Wang, *Catalysis Letters*, 2024, **155**, 11.
Bi05:NiO	1 M KOH	171	85.2	S. Jo, B. Kang, S. An, H. B. Jung, J. Kwon, H. Oh, J. Lim, P. Choi, J. Oh, K.-y. Cho, H.-S. Cho, M. Kim, J.-H. Lee, K. Eom and T. F. Fuller, *ACS Applied Materials & Interfaces*, 2025, **17**, 11946-11955.
Ru-Co_2P@Ru-N-C	1 M KOH	69	65	P. Wang, K. Wang, Y. Liu, H. Li, Y. Guo, Y. Tian, S. Guo, M. Luo, Y. He, Z. Liu and S. Guo, *Advanced Functional Materials*, 2024, **34**, 2316709.
Rh-WO_3	1 M KOH	116	73	N.-A. Nguyen, E. Chuluunbat, T. A. Nguyen and H.-S. Choi, *International Journal of Hydrogen Energy*, 2023, **48**, 32686-32698.
Mo-Ru-B	1 M KOH	50	41	P. Yang, B. Zhou, J. Wang, Y. Wang, Z. Chen, X. Wang, L. Wang, F. Liu and Z. Wu, *International Journal of Hydrogen Energy*, 2023, **48**, 21568-21577.

Table S3. Comparison of recently reported electrocatalysts for HER in 0.5 M H_2SO_4.

HER catalysts	Electrolyte	η_{10} (mV)	Tafel slope ($mV\cdot dec^{-1}$)	Reference
Ru-CoVO-4	0.5 M H_2SO_4	30	53.2	This work
Ru@RuO_2-250	0.5 M H_2SO_4	31	33.5	Z. Li, J. Zou, T. Liang, X. Song, Z. Li, J. Wen, M. Peng, X. Zeng, H. Huang and H. Wu, *Chemical Engineering Journal*, 2023, **460**, 141672.
Mo-Ru-B	0.5 M H_2SO_4	48	34	P. Yang, B. Zhou, J. Wang, Y. Wang, Z. Chen, X. Wang, L. Wang, F. Liu and Z. Wu, *International Journal of Hydrogen Energy*, 2023, **48**, 21568-21577.
Ru-Ru_2P/2D-PCSG-800	0.5 M H_2SO_4	57	44	L. Liu, Z. Wang, X. Zhang, L. Luo and Y. Chen, *Journal of Alloys and Compounds*, 2025, **1010**, 177725.
PW-OA-RuOx@C	0.5 M H_2SO_4	39	57.2-	J. Ding, Z. Peng, Z. Wang, C. Zeng, Y. Feng, M. Yang, G. Hu, J. Luo and X. Liu, *Journal of Materials Chemistry A*, 2024, **12**, 28023-28031.
Rh-WO_3	0.5 M H_2SO_4	48	31	N.-A. Nguyen, E. Chuluunbat, T. A. Nguyen and H.-S. Choi, *International Journal of Hydrogen Energy*, 2023, **48**, 32686-32698.
Co_5Ru_1@NCNT/PF	0.5 M H_2SO_4	45	64	J. Jiao, N.-N. Zhang, C. Zhang, N. Sun, Y. Pan, C. Chen, J. Li, M. Tan, R. Cui, Z. Shi, J. Zhang, H. Xiao and T. Lu, *Advanced Science*, 2022, **9**, 2200010.
RuO_2–WC NPs	0.5 M H_2SO_4	58	66	S.-C. Sun, H. Jiang, Z.-Y. Chen, Q. Chen, M.-Y. Ma, L. Zhen, B. Song and C.-Y. Xu, *Angewandte Chemie-International Edition*, 2022, **61**, e202202519.
Ru-NBC	0.5 M H_2SO_4	40	40.82	Y. Feng, W. Zhu, J. Xu, D. Zhang, Q. Ma, L. Zhao, L. Lin, Q. Su, Y. Wang, Q. Liu, Y. Wei, X. Li, J. Huang, Y. Ye, J. Zhao and B. Wu, *ACS Nano, 2025, **19**, 7948-7961*.
$Ru_{0.10}$@2H-MoS_2	0.5 M H_2SO_4	168	77.5	J. Wang, W. Fang, Y. Hu, Y. Zhang, J. Dang, Y. Wu, B. Chen, H. Zhao and Z. Li, *Applied Catalysis B: Environmental*, 2021, **298**, 120490.
2.20 wt% Ru SAs-Ni_2P	0.5 M H_2SO_4	125	71	K. Wu, K. Sun, S. Liu, W.-C. Cheong, Z. Chen, C. Zhang, Y. Pan, Y. Cheng, Z. Zhuang, X. Wei, Y. Wang, L. Zheng, Q. Zhang, D. Wang, Q. Peng, C. Chen and Y. Li, *Nano Energy*, 2021, **80**, 105467.

Table S4. Comparison of recently reported electrocatalysts for HER in 1 M PBS.

HER catalysts	Electrolyte	η_{10} (mV)	Tafel slope ($mV \cdot dec^{-1}$)	Reference
Ru-CoVO-4	1 M PBS	145	95.81	This work
Ru@RuO_2-250	1 M PBS	43	50.3	Z. Li, J. Zou, T. Liang, X. Song, Z. Li, J. Wen, M. Peng, X. Zeng, H. Huang and H. Wu, *Chemical Engineering Journal*, 2023, **460**, 141672.
Ru - Mo2C@NPC	1 M PBS	170	146.89	Y. Li, Z. Zhang, Y. Yao, Z. a. Wang, Z. Yang, Y. Tong and S. Chen, *Dalton Transactions*, 2024, **53**, 17581-17587.
CoO/Co_3O_4 NA/Ti	1 M PBS	169.8	44.6	Z. Feng, J. Pu, X. Zhang, W. Zhang, M. Liu, L. Cui and J. Liu, *Journal of Alloys and Compounds*, 2021, **881**, 160603.
RuP_2@NC	1 M PBS	196	115.7	B.-Y. Guo, X.-Y. Zhang, J.-Y. Xie, Y.-H. Shan, R.-Y. Fan, W.-L. Yu, M.-X. Li, D.-P. Liu, Y.-M. Chai and B. Dong, *International Journal of Hydrogen Energy*, 2021, **46**, 7964-7973.
Ru@WNO-C	1 M Na_2SO_4	358	139.7	G. Meng, H. Tian, L. Peng, Z. Ma, Y. Chen, C. Chen, Z. Chang, X. Cui and J. Shi, *Nano Energy*, 2021, **80**, 105531.
Ru/Co@NC	0.01 M PBS	286	143	D. Zhao, Z. Li, X. Yu, W. Zhou, Q. Wu, Y. Luo, N. Wang, A. Liu, L. Li and S. Chen, *Chemical Engineering Journal*, 2022, **450**, 138254.
Ni/VN/Ni-NC	1 M PBS	166	109	Q. Liu, K. Liu, X. Li, C. Hui, J. Huang, Z. Deng, D. Yang, L. Cao and L. Feng, *Acs Applied Nano Materials*, 2024, **7**, 4059-4067.
Ru@Ni-MOF	1 M PBS	287	62	L. Deng, F. Hu, M. Ma, S.-C. Huang, Y. Xiong, H.-Y. Chen, L. Li and S. Peng, *Angewandte Chemie-International Edition*, 2021, **60**, 22276-22282.
Ni-Cr-Mo-Fe	1 M PBS	297	94	H. Nady, M. M. El-Rabiei, M. A. Deyab, M. Samy and G. M. Abd El-Hafez, *International Journal of Hydrogen Energy*, 2022, **47**, 39030-39046.
MCNR1	1 M PBS	196	139.09	H. M. C. M. Jayawardana, B. A. Yusuf, S. Meng, Y. Li, H. Ren, Q. Nie, Y. Xu, J. Xie and M. Chen, *Journal of Alloys and Compounds*, 2024, **997**, 174809.

Table S5. Comparison of recently reported electrocatalysts for OER in 1 M KOH.

OER catalysts	Electrolyte	η_{10} (mV)	Tafel slope ($mV \cdot dec^{-1}$)	Reference
Ru-CoVO-4	1 M KOH	220	79.48	This work
Ru-Ni $(OH)_2$	1 M KOH	228	55.2	C. Li, B. Kim, Z. Li, R. Thapa, Y. Zhang, J.-M. Seo, R. Guan, F. Tang, J.-H. Baek, Y. H. Kim, J.-P. Jeon, N. Park and J.-B. Baek, *Advanced Materials*, 2024, **36**, 2403151.
Ru-Co_2P@Ru-N-C	1 M KOH	280	61	P. Wang, K. Wang, Y. Liu, H. Li, Y. Guo, Y. Tian, S. Guo, M. Luo, Y. He, Z. Liu and S. Guo, *Advanced Functional Materials*, 2024, **34**, 2316709.
10%P-RuO_2 NFs	1 M KOH	250	59.9	L. Zhang, W. Li, S. Ren, W. Song, C. Wang and X. Lu, *Advanced Energy Materials*, 2025, **15**, 2403136.
Ru/NF	1 M KOH	235.4	78.98	Y. Hou, Z. Qin, X. Han, Y. Liu, W. Zhang, X. Cao, Y. Cao, J.-P. Lang and H. Gu, *Nanoscale*, 2024, **16**, 6662-6668.
Ru-Fe-Ox/CC	1 M KOH	228	36	M. Shang, B. Zhou, H. Qiu, Y. Gong, L. Xin, W. Xiao, G. Xu, C. Dai, H. Zhang, Z. Wu and L. Wang, *Journal of Colloid and Interface Science*, 2024, **669**, 856-863.
RuO_2/CoFe-LDH/NF	1 M KOH	270	68.3	Q. Chen, Y. Yu, S. Luo, P. Deng, Y. Hua, S. Zhong, X. Tian and J. Li, *International Journal of Hydrogen Energy*, 2024, **84**, 401-409.
SFR30	1 M KOH	334	87.7	W. Zhang, M. Xue, X. Zhang, C. Si, C. Tai, Q. Lu, M. Wei, X. Han, J. Ma, S. Chen and E. Guo, *Applied Surface Science*, 2024, **664**, 160278.
（$Ru_2Fe_2Co_6$）S_2	1 M KOH	248	32.5	Y. Zhu, S. Zhang, R. Chen, Z. Wang, W. Wu, H. Jiang, H. Chen and N. Cheng, *2024, **20**,* 2310611.
$Ru_{0.6}Sn_{0.4}O_2$	1 M KOH	245	61.80	S. Jia, J. Zhang, Q. Liu, C. Ma, Y. Tang and H. Sun, *Journal of Materials Chemistry A*, 2023, **11**, 23489-23497.
Ru-Cl-N SAC	1 M KOH	233	195.1	J. Chen, J. Huang, R. Wang, W. Feng, H. Wang, T. Luo, Y. Hu, C. Yuan, L. Feng, L. Cao, K. Kajiyoshi, C. He, Y. Liu, Z. Li and Y. Feng, *Chemical Engineering Journal*, 2022, **441**, 136078.

Table S6. Overall water splitting performance of the catalyst in 1 M KOH.

catalysts	Electrolyte	η_{10} (V)	stability	Reference
Ru-CoVO-4	1 M KOH	1.46	500h	This work
Ru-Ni $(OH)_2$	1 M KOH	1.53	60h	C. Li, B. Kim, Z. Li, R. Thapa, Y. Zhang, J.-M. Seo, R. Guan, F. Tang, J.-H. Baek, Y. H. Kim, J.-P. Jeon, N. Park and J.-B. Baek, *Advanced Materials*, 2024, **36**, 2403151.
Ru-Co2P@Ru-N-C	1 M KOH	1.56	80000 s	P. Wang, K. Wang, Y. Liu, H. Li, Y. Guo, Y. Tian, S. Guo, M. Luo, Y. He, Z. Liu and S. Guo, *Advanced Functional Materials*, 2024, **34**, 2316709.
Ru/NF	1 M KOH	1.50	24h	Y. Hou, Z. Qin, X. Han, Y. Liu, W. Zhang, X. Cao, Y. Cao, J.-P. Lang and H. Gu, *Nanoscale*, 2024, **16**, 6662-6668.
RuO_2/CoFe-LDH/NF	1 M KOH	1.58	12h	Q. Chen, Y. Yu, S. Luo, P. Deng, Y. Hua, S. Zhong, X. Tian and J. Li, *International Journal of Hydrogen Energy*, 2024, **84**, 401-409.
SFR30	1 M KOH	1.58	24h	W. Zhang, M. Xue, X. Zhang, C. Si, C. Tai, Q. Lu, M. Wei, X. Han, J. Ma, S. Chen and E. Guo, *Applied Surface Science*, 2024, **664**, 160278.
Ru/d-NiFe LDH	1 M KOH	1.49	140h(100 mA cm^{-2})	Y. Chen, Y. Liu, W. Zhai, H. Liu, T. Sakthivel, S. Guo and Z. Dai, *Advanced Energy Materials*, 2024, **14**, 2400059.
(Ru-Co)Ox-350	1 M KOH	1.57	20h	C. Wang, H. Shang, J. Li, Y. Wang, H. Xu, C. Wang, J. Guo and Y. Du, *Chemical Engineering Journal*, 2021, **420**, 129805.
Ru-Cl-N SAC	1 M KOH	1.49	100h	J. Chen, J. Huang, R. Wang, W. Feng, H. Wang, T. Luo, Y. Hu, C. Yuan, L. Feng, L. Cao, K. Kajiyoshi, C. He, Y. Liu, Z. Li and Y. Feng, *Chemical Engineering Journal*, 2022, **441**, 136078.
Ru@MoO$(S)_3$	1 M KOH	1.526	24h	D. Chen, R. Yu, D. Wu, H. Zhao, P. Wang, J. Zhu, P. Ji, Z. Pu, L. Chen, J. Yu and S. Mu, *Nano Energy*, 2022, **100**, 107445.
NCO@RuO2-NCs	1 M KOH	1.5	42	Z. Zhang, X. Liu, D. Wang, H. Wan, Y. Zhang, G. Chen, N. Zhang and R. Ma, *Chemical Engineering Journal*, 2022, **446**, 137037.